VISION
RESEARCH

A Bayesian observer model reveals a prior for natural daylights in hue perception

Yannan Su [a,b,*,1], Zhuanghua Shi [c,2], Thomas Wachtler [a,d,3]

[a] *Faculty of Biology, Ludwig-Maximilians-Universität München, Planegg-Martinsried, Germany*
[b] *Graduate School of Systemic Neurosciences, Ludwig-Maximilians-Universität München, Planegg-Martinsried, Germany*
[c] *General and Experimental Psychology, Ludwig-Maximilians-Universität München, Munich, Germany*
[d] *Bernstein Center for Computational Neuroscience Munich, Planegg-Martinsried, Germany*

ABSTRACT

Incorporating statistical characteristics of stimuli in perceptual processing can be highly beneficial for reliable estimation from noisy sensory measurements but may generate perceptual bias. According to Bayesian inference, perceptual biases arise from the integration of internal priors with noisy sensory inputs. In this study, we used a Bayesian observer model to derive biases and priors in hue perception based on discrimination data for hue ensembles with varying levels of chromatic noise. Our results showed that discrimination thresholds for iso-luminant stimuli with hue defined by azimuth angle in cone-opponent color space exhibited a bimodal pattern, with lowest thresholds near a non-cardinal blue-yellow axis that aligns closely with the variation of natural daylights. Perceptual biases showed zero crossings around this axis, indicating repulsion away from yellow and attraction towards blue. These biases could be explained by the Bayesian observer model through a non-uniform prior with a preference for blue. Our findings suggest that visual processing takes advantage of knowledge of the distribution of colors in natural environments for hue perception.

1. Introduction

The dynamic and statistical nature of the sensory environment poses challenges for sensory processing and perception. Sensory responses to the same stimulus can differ, and different stimuli can cause similar sensory stimulation. However, the natural sensory world is not entirely random but exhibits regularities, and exploiting such regularities can help an organism make useful decisions and efficient actions. Achieving this, however, requires that knowledge about the sensory environment is incorporated in sensory processing.

That sensory processing might utilize knowledge about regularities of the world can be traced back to von Helmholtz's idea of 'unconscious inference' (von Helmholtz, 1867). In recent decades, the development of the Bayesian inference framework suggests that incorporating prior knowledge can significantly enhance the reliability of perceptual estimation, especially when the input signals are corrupted by noise (Knill & Pouget, 2004; Shi et al., 2013). The Bayesian inference framework has successfully accounted for perceptual performance in object perception (Kersten et al., 2004), multi-sensory integration (Ernst & Banks, 2002), sensorimotor learning (Körding & Wolpert, 2004), visual speed perception (Stocker & Simoncelli, 2006), visual orientation perception (Girshick et al., 2011; Su et al., 2023), and time perception (Shi & Burr, 2016; Glasauer & Shi, 2022).

In the case of orientation perception, Bayesian approaches have revealed that human observers' perceptual judgments are systematically biased towards cardinal orientations (Girshick et al., 2011). The corresponding prior matched the non-uniform distribution of orientation in natural scenes, where orientations near the cardinals have a higher incidence than oblique orientations (Girshick et al., 2011). Non-uniformities in the statistics of natural sensory signals also exist in the domain of color. For example, distributions of cone-opponent signals in natural scenes show a correlation between S-(L + M) and (L-M) co-ordinates (Webster & Mollon, 1997; Wachtler et al., 2001; Nascimento et al., 2002; Webster et al., 2007), indicating a dominance of contrasts

along an oblique color space axis that corresponds to the variation of natural daylights. Analyzing human color perception in a Bayesian framework may provide insights into how human color perception is adapted to such non-uniformities in the chromatic properties of the natural environment.

In the Bayesian framework, an observer's statistical inference is influenced by two key components: the likelihood, which is the probability of sensory measurements given a stimulus, and the prior, which reflects the observer's prior knowledge about stimulus probabilities (Knill & Pouget, 2004). Optimal integration of the two components results in a posterior density function that represents the probability of the stimulus given the measurements. Common choices for an optimal observer when selecting a point estimate of the posterior include the mode (maximum a posterior, MAP) or the mean (Stocker & Simoncelli, 2006).

A common difficulty encountered in the Bayesian inference framework lies in measuring likelihood and prior, which are not directly accessible. Stocker and Simoncelli (2006) proposed a method to recover likelihood and prior from psychophysical measurements of perceptual bias and variability. Specifically, these measurements were obtained from discrimination between stimuli with different noise levels, corresponding to different widths of the likelihood. According to the Bayesian inference framework, this results in different posterior distributions. When the likelihood does not align with the prior, the larger the noise, the larger the shift in the posterior induced by the prior (Fig. 1). Girshick et al. (2011) used this approach to investigate orientation perception and revealed a prior that peaked at the cardinal orientations, suggesting that visual perception may involve prior information regarding the regularities of natural scene structures.

To investigate how prior knowledge is integrated into color processing, we closely followed the approach by Stocker and Simoncelli (2006) and Girshick et al. (2011), applying the Bayesian framework in hue perception. We measured perceptual variability and biases of observers in the discrimination of noisy hue ensembles and used a Bayesian model to recover their priors.

2. Methods

2.1. Participants

Six observers, (two males and four females), ranging in age from 23 to 56 years, participated in the experiments. Four of the subjects had no knowledge with respect to the purpose of the study, while two were authors. All had normal or corrected-to-normal vision. Participants signed informed consent prior to the experiment and received a compensation of 10 Euros per hour. The study was conducted in accordance with the Declaration of Helsinki.

2.2. Stimuli

Stimuli were presented on a ViewPixx Lite 2000A display (VPixx, Saint-Bruno, QC, Canada), calibrated by a PR-655 spectroradiometer (PhotoResearch, Chatsworth, CA, USA) and controlled by a Radeon Pro WX 5100 graphics card (AMD, Santa Clara, CA, USA) in a HP Compaq Elite 8300 desktop computer running Ubuntu Linux 20.04. The screen resolution was set to 1920×1200 pixels at a refresh rate of 120 Hz. Stimuli were generated using PsychoPy 2020.1.2 (RRID:SCR_006571, Peirce et al., 2019) based on Python 3.6 (RRID:SCR_008394).

Chromaticities of the stimuli were defined in an opponent cone contrast color space, similar to the one used by Derrington et al. (1984), but with the polarity of the y-axis defined such that positive values corresponded to increasing S-cone stimulation, in line with MacLeod and Boynton (1979). The x-axis corresponded to increasing L-cone excitation and decreasing M-cone excitation (L-M), such that the sum of L and M remained constant. Cone excitations were estimated based on the Stockman and Sharpe (2000) cone fundamentals. Cone contrasts were calculated with respect to a neutral gray (CIE [x, y] = [0.307, 0.314], 106.7 cd/m^2), which also served as the display background on which stimuli were presented and to which subjects were adapted. The cone excitations corresponding to this reference gray served as starting values from which resulting cone excitations for a given stimulus were calculated according to its cone contrasts. L-M cone contrasts were measured as the sum of the contrast of L and M cones. S-cone contrasts were scaled by a factor of 2.6, yielding approximately equally salient stimuli for all hues at a given cone contrast (Teufel & Wehrhahn, 2000).

To account for individual differences in luminance perception, the color space plane that each subject perceived as isoluminant with the reference gray was determined using the method of Teufel and Wehrhahn (2000). Isoluminance points for 16 stimuli of different hues were determined using heterochromatic flicker photometry (Kaiser & Boynton, 1996). Fitting a plane through the reference gray to these data yielded an estimate of the individual isoluminant plane for the respective observer. The individual luminance corrections relative to the nominal isoluminant plane were less than 4%.

All stimuli used were isoluminant and had a fixed cone contrast of c = 0.12 with respect to the neutral gray background. Thus, stimuli varied only in azimuth angle, corresponding to hue (Fig. 2a). Note that scaling the S axis with respect to the L-M axis will affect the numerical values of hue angles for stimuli not aligned with a coordinate axis, but will not change their respective quadrants in the isoluminant plane. Each stimulus presentation consisted of a reference stimulus, a comparison stimulus, and a color gradient bar as a hue sequence reference (Fig. 2b). This color gradient was introduced to provide a direction of hue change, because, in contrast to orientation judgments, for hue there is no perceptual quality corresponding to clockwise vs. counterclockwise rotation. The gradient bar indicated from left to right increasing hue
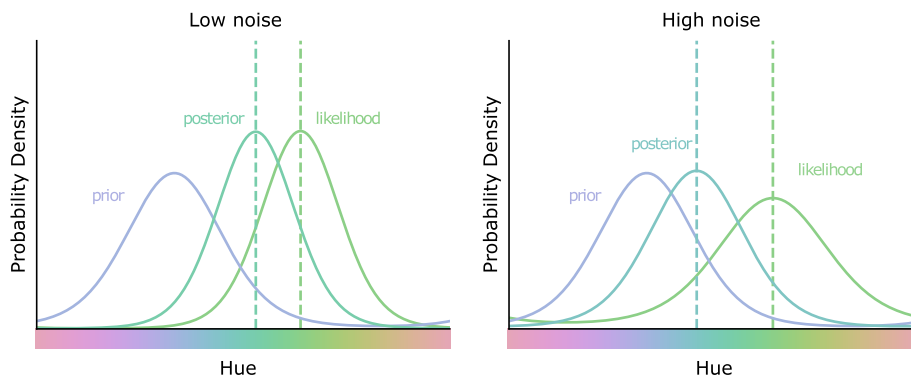

Fig. 1. Illustration of Bayesian inference in hue perception (after Stocker and Simoncelli, 2006). The same prior integrates with the likelihoods for two stimuli with different noise levels. Left: A stimulus with a low level of noise results in a narrow likelihood and thus a small shift of the posterior. Right: A stimulus with a high level of noise results in a wide likelihood and thus a large shift of the posterior.
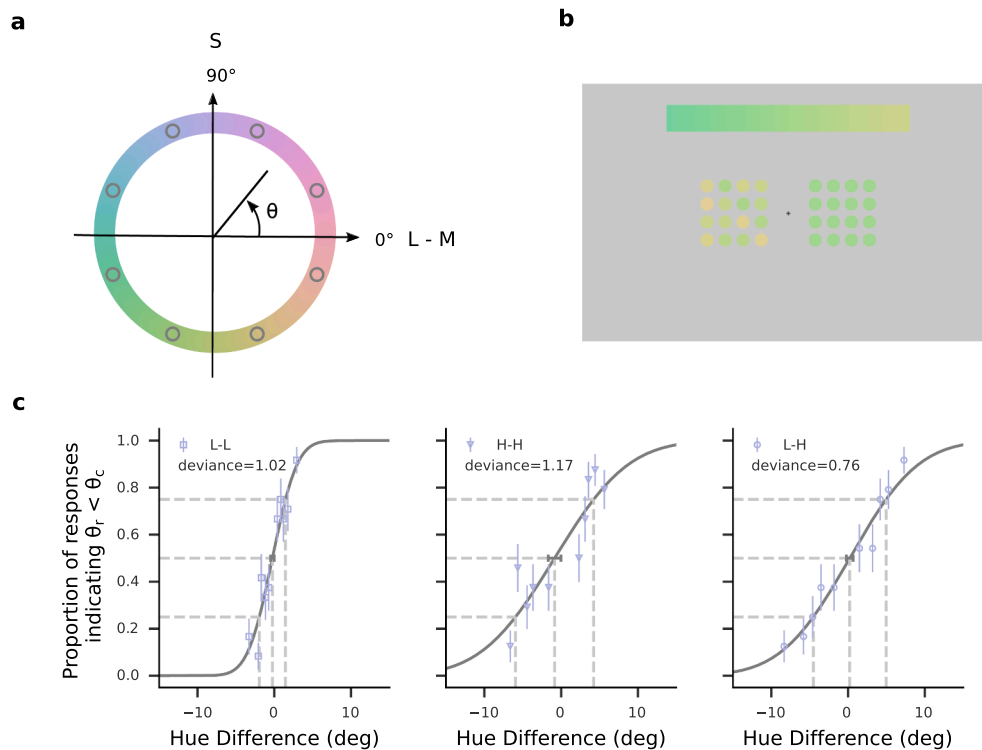
Fig. 2. Stimuli and psychometric functions. (a) Stimulus chromaticities. All stimuli were defined in the isoluminant plane with fixed chromatic contrast and thus varied only in azimuth angle, corresponding to hue (colored circle). Eight hues with equidistant azimuth angles θ (gray open dots) were defined as reference hues. (b) Example of a stimulus display. Participants were asked to compare two arrays of color patches, presented on the left and right sides of fixation, and to indicate whether their respective average hues matched the direction of hue changes that was indicated by the color gradient bar at the top of the display. (For this example, the correct response should be 'No', given that the hue averages of the arrays from left to right do not match the direction of hue changes indicated by the color gradient bar). The figure shows the cross-noise condition with a high-noise array on the left and a low-noise array on the right. Note that hue differences have been exaggerated in the figure for illustrative purposes. (c) Examples of psychometric functions for the three noise conditions. Proportions of responses indicating the subject perceived the hue angle of the comparison stimulus (θ_c) as larger than the hue angle of the reference stimulus (θ_r) are plotted as a function of the difference between the hue angles θ_c and θ_r. Data are from a single subject's responses with $\theta_r = 112.5°$ for the three noise conditions L-L (left), H-H (center), and L-H (right). Error bars of the data points denote standard error. Solid lines show cumulative Gaussian functions fitted to the data. Dashed lines denote 25%, 50%, and 75% values. Horizontal error bars around the estimated 50% points denote 68% confidence intervals. Deviance values represent the goodness of fit.

changes along the color space azimuth (Fig. 2a-b). Both reference and comparison stimuli consisted of arrays of 16 circular patches with diameters of 0.75° of visual angle, evenly spaced on a 4 × 4 grid extending 3° × 3° of visual angle. Within each stimulus, the circular patches were randomly positioned on the grid of the array. The color gradient bar had an extent of 12° × 1.5° of visual angle.

On a neutral gray background (46.01° × 29.68°), a fixation cross (0.6° × 0.6°) was presented at the screen center. The color gradient bar was presented on the upper part of the screen, 5° above the center. Reference and comparison stimuli were placed 3° left and right from the fixation cross, with the sides of reference and comparison stimulus assigned trial-by-trial in a pseudo-random fashion such that their positions were balanced within each session.

For both reference and comparison stimuli, the hues of the circular patches either were identical (low-noise stimuli) or were drawn from a uniform distribution with a range (noise level) that was individually pre-determined for each subject to yield thresholds twice as large as the low-noise stimuli (high-noise stimuli, see below). The reference hues, θ_r, were evenly spaced along the azimuth of color space at 45° intervals from 22.5° to 337.5°. For each θ_r, the corresponding color gradient bar was filled by 45 evenly spaced hue angles from θ_r - 30° to θ_r + 30°.

2.3. Procedures

During the experiment, the participant sat in a dimly lit room and viewed the display binocularly from a viewing distance of 57 cm. A central fixation cross was displayed and participants had to maintain

their eyes on the fixation throughout the entire trial.

Each trial started with the presentation of the color gradient bar to indicate the range of hues to be tested. After 500 ms, the reference stimulus and the comparison stimulus were presented simultaneously for 500 ms, followed by a 500-ms full-screen checkerboard pattern of random chromatic squares (1.3° × 1.2°) to prevent afterimages of the stimuli. Participants were instructed to compare the two stimuli and indicate whether the ensemble hue averages of the arrays from left to right matched the direction of color change shown by the color gradient bar. Responses were given by pressing the up or down arrow key with the right hand. There was no time constraint on the response. Average response times were within one second.

For a given reference stimulus, its average hue and corresponding color gradient bar remained unchanged across trials, while the absolute hue difference between the reference hue and the average hue of the comparison stimulus was adjusted by a 1-up/2-down staircase that increased the absolute hue difference after every incorrect response and decreased the absolute hue difference after every two consecutive correct responses. Note that, for a given reference, there were two independent 1-up/2-down staircases to adjust the comparison stimuli whose average hues were smaller and larger than the reference, respectively. Two same-noise conditions, low-noise versus low-noise (L-L) and high-noise versus high-noise (H-H), and one cross-noise condition, low-noise versus high-noise (L-H), were tested in the experiments. In the cross-noise condition, the reference stimulus was always the low-noise stimulus.

Following the approach of Girshick et al. (2011), prior to the main

experiment, we determined each participant's level of hue variance for the high-noise stimulus, ensuring the H-H discrimination thresholds were about twice as large as L-L discrimination thresholds. We selected a reference hue angle of $135°$, as thresholds for this hue were at intermediate levels. For each participant, we measured the discrimination threshold (d_L) of this stimulus in the L-L condition by fitting a cumulative Gaussian function to the psychophysical data. Next, we fixed the reference and comparison stimuli at $135°$ and $135° + 2d_L$, respectively, adjusting the hue noise of both stimuli using a 1-up/2-down staircase to achieve 75% accuracy based on the psychometric function. The determined noise levels ($21.2°, 20.1°, 24.5°, 20.1°, 22.2°$, and $24.4°$ for the six subjects, respectively) were used for the high-noise stimuli in the main experiment. Note that these measurements were only used to determine the hue variances and excluded from other analyses.

In the main experiment, each session consisted of 128 trials, in which the first 8 trials were warm-up trials with random hues and were excluded from further analysis. Within each session, two reference stimuli with $180°$ difference in their mean hue angles, were randomly interleaved. Prior to the formal experiment, participants completed four practice sessions with feedback about the correctness of their responses given as text emojis (":)" or ": (" for correct and incorrect responses, respectively). The feedback was only given in the practice sessions but not in the formal experiment. Each participant performed 5760 trials divided into 24 conditions (8 reference stimuli × 3 comparison conditions) over 48 sessions.

2.4. Data analysis

2.4.1. Estimation of perceptual variability and bias

The psychophysical data were analyzed separately for each subject. In addition, data for a hypothetical average observer were obtained by pooling all subjects' data. For the data of each condition, we fitted a cumulative Gaussian function (Fig. 2c) using non-linear least square minimization with the Nelder-Mead algorithm (Gao & Han, 2012) and determined its mean, representing the point of subjective equality (PSE) and the standard deviation, representing the just noticeable difference (JND). PSE and JND thus reflected perceptual bias and perceptual variability, respectively.

2.4.2. Estimation of the measurement distributions and the likelihood functions

The measurement distribution is the conditional distribution $p(m|\theta)$ and corresponds to the likelihood of a sensory measurement m given a particular stimulus hue angle θ. For each stimulus θ we estimated the measurement distribution as a von Mises distribution with a peak at θ and the concentration parameter κ_θ, thus

$$p(m|\theta) = \frac{e^{(\kappa_\theta \cos(\theta - m))}}{2\pi i_0(\kappa_\theta)}, \tag{1}$$

where $i_0(\kappa_\theta)$ is the modified Bessel function of order 0. The concentration parameter κ_θ represents the measurement noise and is converted from the corresponding perceptual variability $J(\theta)$ by $\kappa_\theta = J^{-2}(\theta)$. For each same-noise condition (L-L and H-H),we estimated $J(\theta)$ by fitting each subject's JNDs as a sine mixture function of the hue angle θ:

$$J(\theta) = a(\sin\theta + \sin 2\theta) + b. \tag{2}$$

With periods of $180°$ and $360°$, the two sine functions allow capturing both the periodicity and asymmetry of the JND patterns. The parameters a and b were estimated using non-linear least squares minimization.

To avoid any constraint of predefined shapes in estimating the likelihood, we adopted a sampling method based on representing the measurement distribution and the likelihood function as a two-dimensional function (Girshick et al., 2011), where the vertical dimension represented measurement distributions centered on particular stimulus hue angles θ, and the horizontal dimension represented likelihood functions of θ given particular measurements m. Thus, a single measurement from the measurement distribution resulted in a likelihood given by the corresponding horizontal slice of the two-dimensional function.

2.4.3. Estimation of the priors

To estimate the prior, we considered unimodal as well as alternative multimodal models. As model of the unimodal prior $p(\theta)$ we chose a von Mises function (Eq. 1), which guarantees that the prior had a period of $360°$ and an integral of 1. We determined the prior by fitting the estimation of a Bayesian observer to the behavioral data under the cross-noise condition (Girshick et al., 2011). We assumed that the Bayesian observer encodes with sensory noise and gives distributed measurements $m(\theta)$ for repeated presentation of the same stimulus θ. Each measurement leads to a likelihood function, which is multiplied by the prior to obtain a maximum a posterior (MAP) estimate at the decoding phase. Note that, an alternative to the MAP estimate is the mean of the posterior; however, we opted for the MAP estimate in alignment with the approach outlined by Girshick et al. (2011). The MAP estimate thus represents the observer's estimate $\hat{\theta}$ of the stimulus θ. Therefore, the measurement distribution of a stimulus results in a distribution of MAP estimates. The discrimination task was simulated by comparing two MAP estimate distributions according to signal detection theory (Green & Swets, 1966), yielding a single point on the simulated psychometric function.

According to the Bayesian inference framework, non-negligible biases reflecting the prior should only be observed in the cross-noise condition in our experiments (Fig. 1). Thus, we fitted the observer model to the cross-noise biases to obtain the optimal parameters of the prior. For each participant, we simulated 1000 trials for each stimulus pair of the cross-noise comparison data. For every paired low-noise and high-noise stimuli, 1000 samples each were drawn from two corresponding measurement distributions with centers at m_L and m_H, and concentration parameters κ_L and κ_H, respectively. Each sample generated a likelihood function that was combined with the prior and led to an estimate of the stimulus. The two distributions formed by the 1000 estimates each were compared, resulting in a response probability given the corresponding stimulus pair. We then obtained a model-generated psychometric function by fitting a cumulative Gaussian function to the simulated data.

We evaluated the prior model by computing the likelihood of the cross-noise data given the model-generated psychometric function. The optimal parameters of the prior for each subject were estimated by maximizing the overall likelihood. We performed bootstrapping on each subject's binary responses for each stimulus pair 100 times and estimated the priors given the bootstrapped data. The point-wise standard deviation of the 100 estimated priors was taken as the uncertainty of the estimates. We further assessed the model by comparing its performance with the performance of a model with a uniform prior. We evaluated the performance of the model by a normalized difference of log-likelihood to the model with the uniform prior,

$$L = \frac{L_{est} - L_{uni}}{L_{raw} - L_{uni}}, \tag{3}$$

where L_{est} and L_{uni} represent the log likelihoods of the models with the estimated prior and the uniform prior, respectively, and L_{raw} represents the log likelihoods of the raw psychometric fits. Thus, $L = 0$ corresponds to the model with a uniform prior and $L = 1$ corresponds to the raw psychometric fits. Given the difference in the degrees of freedom between the estimated prior and the uniform prior, we also calculated the Akaike Information Criterion (AIC) scores (Akaike, 1998) of the models.

To validate the unimodality of the prior model, we also modeled two alternative priors by normalized sine functions with periods of $360°$ and $180°$, respectively, and determined the prediction performance of the

observer models with these priors. While we cannot exclude the possibility of other forms of alternative priors, the 180° sine model enables describing multimodal priors while keeping the number of parameters well below the number of sample points in our data. Furthermore, perceptual quantities such as thresholds and biases often show symmetries in color space (Danilova & Mollon, 2010; Klauke & Wachtler, 2015), and our data of variability and bias (see Results) were in line with such symmetry. Therefore, a prior with 180° periodicity seems the most promising model for a multimodal prior.

3. Results

3.1. Behavioral results

We used two-alternative forced-choice discrimination experiments to measure perceptual variability and bias in hue perception. We tested three conditions for each measured hue: two same-noise conditions (low-noise versus low-noise, L-L, and high-noise versus high-noise, H-H), and one cross-noise condition (low-noise versus high-noise, L-H). The purpose of adopting these conditions was grounded in the Bayesian inference framework, which posits that, assuming the same prior, biases would not differ between stimuli with the same noise level but would increase with the noise level (Fig. 1). Thus, the same-noise conditions enabled measuring the perceptual variability of stimuli with specific noise levels, while the data in the cross-noise condition could potentially reveal the effect of a prior through a cross-noise bias, that is, a difference between the low- and the high-noise bias.

We fitted the psychometric data for hue discrimination across varying noise conditions with cumulative Gaussian functions (see Fig. 2c for examples). The goodness of the psychometric fit was measured by deviance (Wichmann & Hill, 2001) and was comparable across subjects (0.94 ± 0.38 for the L-L condition, 1.03 ± 0.34 for the H-H condition, and 1.17 ± 0.61 for the L-H condition). Based on the estimated psychometric function, we used the standard deviation of the cumulative Gaussian function as the just noticeable difference (JND) and calculated the point of subjective equality (PSE) at the threshold of 50%. These values reflected the discrimination thresholds and bias of each participant, respectively. In addition, we determined the results for a hypothetical average subject whose data were from pooled trials of all subjects. This average subject showed an average performance: there was no significant difference between the average subject's psychophysical estimates and the mean values of all subjects' psychophysical measurements (sign test $p = 0.44$ for discrimination thresholds, sign test $p = 0.68$ for biases).

3.1.1. Discrimination thresholds

Under the same-noise conditions, discrimination thresholds as a function of hue angle typically exhibited a bimodal pattern (Fig. 3a). On average, across subjects, the L-L condition had two local minima at hue angles of $101.3° \pm 22.5°$ and $298.1° \pm 28.8°$ (see Figs. S1 and S2), and two local maxima occurred at $49.5° \pm 24.6°$ and $170.4° \pm 21.9°$. Fitting a sine mixture model to the discrimination thresholds yielded similar hue angles corresponding to these extrema (local minima at $97.3° \pm 28.4°$ and $290.7° \pm 18.1°$, and local maxima at $39.4° \pm 47.1°$ and $186.7° \pm 23.6°$, averaged across subjects; Fig. 4a-b, also see Fig. S4a).

The bimodal pattern of discrimination thresholds, with the lowest thresholds near an oblique blue-yellow axis, is in line with the results of previous studies (Danilova & Mollon, 2010; Witzel & Gegenfurtner, 2013). In the H-H condition, thresholds were significantly higher than in the L-L condition (sign test $p < .001$) but the bimodal pattern persisted, however two of the subjects (S2 and S6) showed inconsistent maxima and minima between the conditions (Fig. S1). The cross-noise condition (L-H) typically yielded intermediate discrimination thresholds (Fig. 3b). Of the L-H discrimination thresholds, 82.5% were higher (sign test $p < .001$) than the corresponding L-L discrimination thresholds, and 90.0% were lower (sign test $p < .001$) than the H-H discrimination
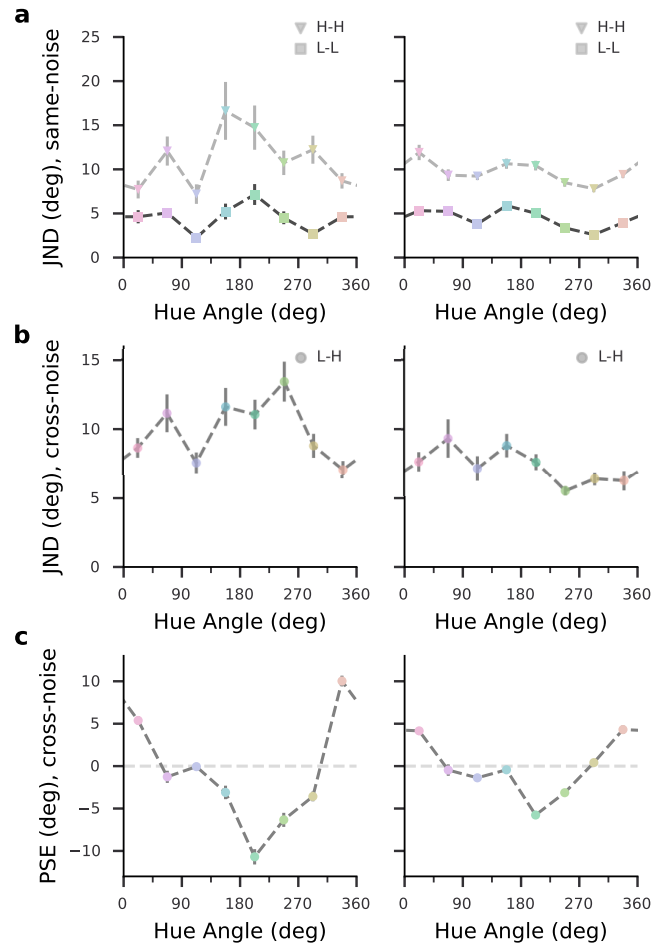
Fig. 3. Experimental data for subject S3 (left) and the average subject (right). (a) Hue discrimination thresholds (JNDs) under the same-noise condition. (b) Hue discrimination thresholds under the cross-noise condition. (c) Biases under the cross-noise condition, measured as hue angle differences between the high-noise and low-noise stimuli at the PSE. Bars denote one standard error of the estimates.

thresholds.

3.1.2. Biases

We observed non-negligible bias only under the cross-noise condition (L-H) for all subjects (Fig. 3c; also see Fig. S3 for the same-noise bias results), which matches our prediction based on the Bayesian inference framework: assuming the same prior for perceptual inference, biases would only differ among stimuli with different noise levels. Given that in the cross-noise condition the low-noise stimulus always served as the reference stimulus, with fixed hue across trials, the cross-noise bias shown in Fig. 3c represents the perceptual bias of the high-noise stimulus relative to the low-noise stimulus. Averaged across subjects, the biases showed a minimum of $-5.6° \pm 3.1°$ and a maximum of $5.5° \pm 2.9°$. Among the biases, 88.9% of the negative values corresponded to hue angles within the range of 112.5° to 292.5°, and 85.7% of the positive values were at the hue angles smaller than or equal to 112.5°, or larger than or equal to 292.5°, which indicated bias zero-crossings along an oblique blue-yellow axis. Specifically, zero-crossings occurred at the hue angles within 45° around 112.5° and within 45° around 292.5°, except for one subject whose zero-crossings did not fall within the hue angles of 112.5° ± 45°. Around the zero-crossings, biases were attractive towards blue hues (near 112.5°) and repulsive away from yellow hues (near 292.5°). Most subjects exhibited two zero-crossings, around 112.5° and 292.5°, respectively. The two
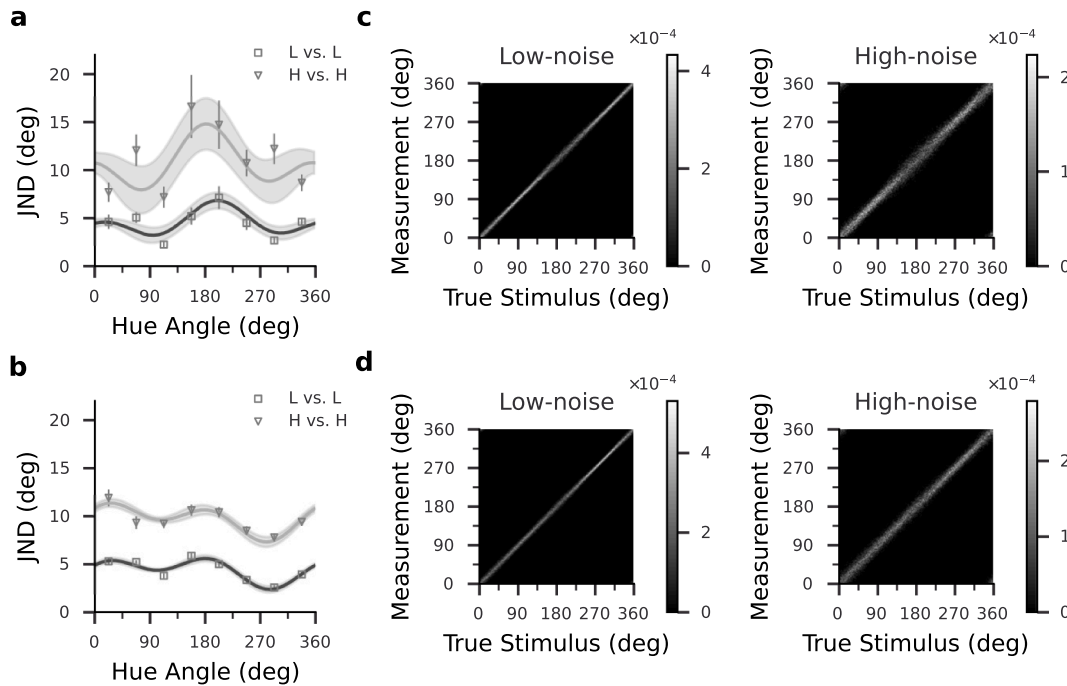
Fig. 4. Threshold fits and estimated likelihood functions in the same-noise conditions. (a and b) Fitted JNDs of subject S3 (a) and the average subject (b). JND estimates are from the data shown in Fig. 3, error bars indicate one standard error. The dark and light gray lines are the fitted JNDs for the L-L and the H-H conditions, respectively. The gray shaded area indicates 68% confidence intervals of fitted JNDs. (c and d) Estimated likelihood functions of subject S3 (c) and the average subject (d). Each horizontal slice of the two-dimensional function represents a likelihood function of stimulus hue angle θ given a particular measurement m, and each vertical slice represents a measurement distribution centered on a particular θ. The gray level represents corresponding probability densities.

subjects that had inconsistent discrimination thresholds across conditions showed additional bias zero-crossings around 157.5° (see S2 and S6 in Fig. S1). According to the Bayesian observer model, perceptual bias arises when the prior is non-uniform over the stimulus space and misaligned with sensory measurements. This prediction matches our observations of non-zero cross-noise bias, suggesting non-uniformity of the perceptual prior.

Since our color space is not perceptually uniform, we expect some bias to arise from the variation of discrimination thresholds. If changes in thresholds occur over a scale of hue angles comparable to the hue range of the noisy stimulus arrays, then the perceived ensemble average for a given stimulus may vary depending on the noise level. To determine the contribution of threshold non-uniformities to observed bias, we simulated the effect of non-uniform thresholds when the paired cross-noise stimuli had identical central hues of the ensemble. For each subject, we multiplied the hue angle differences between the hues in the high-noise stimuli and the central hue of the ensemble by the inverse of the fitted JNDs (see Modeling Results and Fig. 4a-b). Thus, we mapped the stimuli to a scale where hue differences were represented as multiples of discrimination thresholds and then computed the hue averages of the scaled stimuli. This resulted in biases that varied systematically with hue angle, corresponding to the variation in discrimination thresholds. However, their magnitudes were considerably smaller than the observed cross-noise bias (Fig. S1). Averaged across observers, the biases arising from threshold non-uniformities showed maximal magnitudes of $0.91° \pm 0.78°$, that is, less than 20% of the magnitudes of the experimentally measured biases. Thus, the variation of discrimination thresholds had a negligible influence on the cross-noise biases.

Taken together, we found that hue discrimination thresholds followed a bimodal pattern, with observers showing the best discrimination for bluish and yellowish stimuli. The introduction of chromatic noise resulted in increases in discrimination thresholds and cross-noise biases. The observed biases were attractive towards blue and repulsive from yellow, indicative of non-uniform priors.

3.2. Modeling results

To determine priors employed by observers, we used a Bayesian ideal observer model and optimized prior parameters to predict behavioral hue judgments. The model connects two behavioral measurements—discrimination threshold and bias—to two Bayesian components—likelihood and prior. Specifically, the stimulus uncertainty was propagated from the measurement distribution to the posterior distribution, resulting in perceptual variability (Girshick et al., 2011). In line with this model, measurement distributions and likelihood functions were computed from the fitted same-noise variabilities. When stimulus noise increased the threshold, the widths of the corresponding measurement distribution and likelihood function were also increased (Fig. 4, see also Fig. S4). We assumed the ideal observer's estimates of a particular stimulus θ corresponded to maximum a posteriori (MAP) estimates $\widehat{\theta}$ resulting from multiplying the likelihood function with a prior at the Bayesian decoding stage. We simulated each subject's cross-noise data by comparing each pair of MAP estimate distributions ($\widehat{\theta}_L$ and $\widehat{\theta}_H$). The prior was modeled as a von Mises function, and the prior parameters were obtained by maximizing the likelihood of the experimental data given the simulation-generated psychometric function.

Most individual subjects' priors, as well as the prior of the average subject, peaked in the second quadrant, corresponding to positive S and M cone contrasts and negative L cone contrast, that is, colors that appear bluish. These priors were large and had comparatively narrow peaks with standard deviations between 19.3° and 33.1° (Fig. 5 and Fig. S5). The two subjects whose discrimination thresholds were inconsistent across noise levels and whose biases showed more than two zero crossings had priors that peaked in the fourth quadrant (Fig. S5). These priors were shallow and relatively broad, with standard deviations of 37.7° and 48.4°. None of the priors peaked in the first or third quadrant.

The confinement of priors to the second and fourth quadrants is in line with both the distribution of natural spectra and perceptual properties. Natural spectra vary mainly along the daylight locus, which
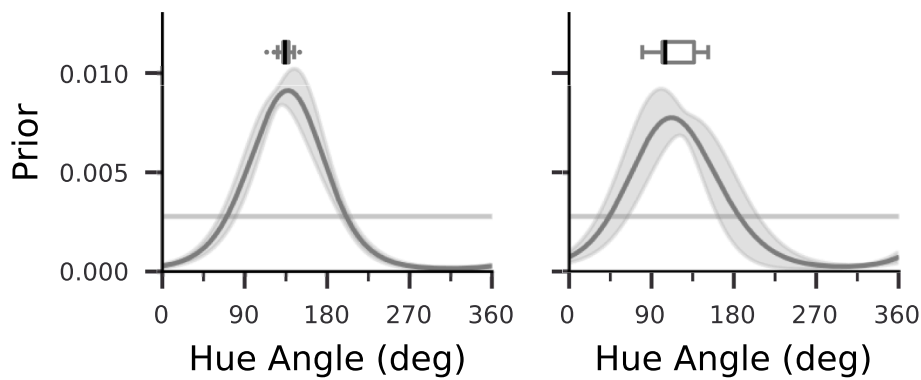
Fig. 5. Estimated prior for subject S3 (left) and the average subject (right). The gray shaded area indicates the point-wise standard deviation of 100 bootstrapped estimates. The boxes above the curves indicate the first quartile to the third quartile of the peak locations of the 100 bootstrapped estimates, with the black line at the median. The whiskers extend from the box by 1.5× the inter-quartile range (IQR). Flier points indicate values beyond the range of the whiskers. The light gray horizontal line represents the uniform prior.

covers the range from long-wavelength-dominated sunlight to short-wavelength-dominated light from the blue sky (Wyszecki & Stiles, 1982). The daylight locus aligns closely with a perceptual blue-yellow axis connecting wavelengths of 476 nm and 576 nm on the spectral locus (Mollon, 2006). This axis has an angle of 112° in our color space. The cross-subject average of the hue angles of prior peaks was 107.3° ± 26.7° (SE). The estimated prior for the average subject had its peak at 115.2° ± 19.9° (Fig. 5, right).

The elongation of the distribution of natural colors along an oblique axis in color space is paralleled by a perceptual non-uniformity: Discrimination thresholds are higher along this axis than perpendicular to it. This relation between natural stimulus statistics and perception is nicely illustrated by comparing the color gamut of natural scenes and colors from the Munsell palette plotted in the same color space (see Fig. 5 in Webster, 2020). The distribution of our priors is in line with this picture, while at the same time emphasizing an asymmetry in favor of blue over yellow.

To assess the effectiveness of the encoding–decoding model with the estimated prior, we compared its performance in predicting the cross-noise bias against a model with a uniform prior. The model with the estimated prior was found to be better at predicting both the sign and amplitude of the cross-noise bias than the model with the uniform prior (Fig. 6a-b). Across all subjects, the normalized log-likelihoods indicated that the estimated prior outperformed the uniform prior (Fig. 6c). Furthermore, when comparing the two prior models using Akaike Information Criterion (AIC) scores (Akaike, 1998), we found that the estimated prior consistently performed better than the uniform prior

(Table S1). Additionally, modeling the prior as a normalized sine function yielded similar results, with the estimated prior peaking around the blue hue (119.1° ± 28.6° (SE), averaged across subjects, see Fig. S7). Note that the sine function had a constrained period of 360° and thus exhibited a single peak over the hues. Its prediction performance was better than a bimodal sine function with period 180° (Fig. S7), which confirmed the unimodality of the prior.

In summary, these results indicate that the observers used a non-uniform prior related to the oblique blue-yellow axis. Specifically, the average prior showed the highest probability at blue and the lowest probability at yellow.

4. Discussion

Our study aimed to investigate the perceptual characteristics of hue discrimination and identify an internal prior that contributes to hue perception. The experimental results showed that the lowest discrimination thresholds and smallest biases occurred for stimuli near a perceptual blue-yellow hue axis. In addition, cross-noise perceptual biases were attractive towards blue and repulsive from yellow, which was explained by a Bayesian observer model with a prior that favored blue. Our study extends the Bayesian perspective on perception to the domain of color and provides evidence of a systematic bias in color perception related to natural daylights. In contrast to previous attempts, where it had turned out difficult to determine adequate priors to explain human performance in color judgments (Brainard et al., 2006), our study presents an approach that recovers a prior that explains hue
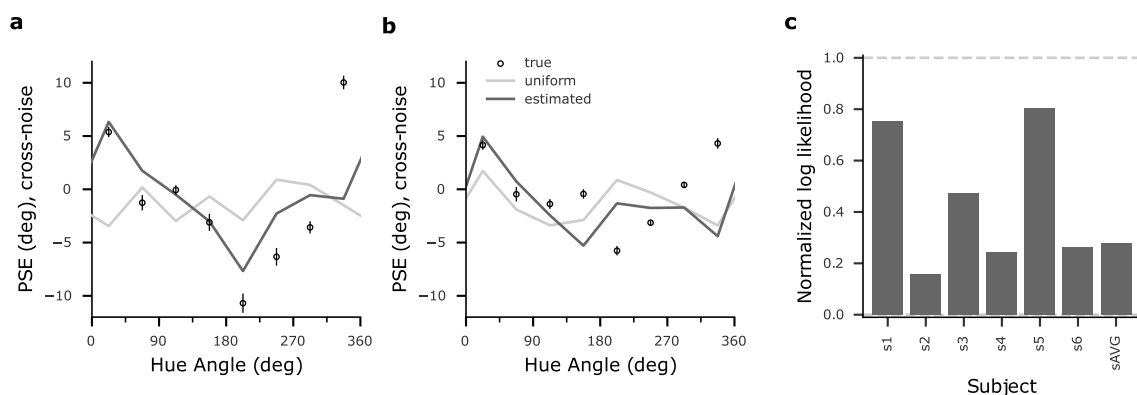

Fig. 6. Comparison of priors. (a and b) Cross-noise biases with predictions from estimated prior (black lines) and uniform prior (gray lines) for subject S3 (a) and the average subject (b). Circles represent the cross-noise biases shown in Fig. 3. (c) Normalized log-likelihoods of predictions using the estimated prior for all subjects, including the average subject (sAVG). Values greater than 1 indicate prediction better than raw psychometric fits, and values greater than 0 indicate prediction better than the model with uniform priors.

perceptual bias and can be related to natural color statistics.

Our investigation focused on the hue aspect of color perception, using an isoluminant hue circle with fixed cone contrast. However, color perception also includes brightness and saturation, which vary along the luminance axis and with radial distance in the isoluminant plane, respectively. Thus, our results should be seen as reflecting a one-dimensional aspect of a broader multi-dimensional prior for color perception. For context-induced biases, there is a consistent generalization from one dimension to higher dimensions in color space (Klauke & Wachtler, 2015; Vattuone et al., 2021; Vattuone & Samengo, 2023), and we expect the same for biases arising from a prior and the prior itself. While it may be difficult to practically determine the prior distribution along the saturation dimension (i.e., the radial direction in the color space), it is quite possible that the actual three-dimensional prior has a peak at a luminance level different from isoluminance. The main axes of variation of natural spectra vary in elevation, but not systematically with hue (Webster & Mollon, 1997). Therefore, had we included stimuli with luminance variations and recovered the two-dimensional distribution of the projection of the prior onto the unit sphere, its actual peak might lie outside the horizontal isoluminance plane. However, we would not expect a significant difference in the azimuth value.

4.1. Ensemble hue perception and interindividual variability

Our psychophysical results showed that subjects could effectively integrate the information over noisy hue ensembles, which agrees with previous findings on ensemble hue perception (Maule et al., 2014; Webster et al., 2014; Maule & Franklin, 2015; Virtanen et al., 2020). Specifically, our data confirm that hue averaging does not require a spatial configuration with abutting hue elements (Virtanen et al., 2020).

Previous studies have indicated that categorical effects may influence the percept of hue ensembles (Maule et al., 2014). However, discrimination thresholds in our experiments were approximately equal between yellow and blue ($p = 0.35$), despite their categories spanning different hue angle ranges (Webster et al., 2000; Hansen et al., 2007; Witzel & Gegenfurtner, 2013). Moreover, observers were instructed to discriminate hue using an external physical reference instead of internal criteria, minimizing potential categorical effects from subjective color naming. Nevertheless, to identify any relationship of the priors with individual specifics in color vision, we compared the locations of priors and unique hue percepts of the individual subjects. We determined the unique hue locations in five subjects (see Supplementary Methods) and found the standard deviation in unique hue locations ($5.31° \pm 2.05°$, averaged across four unique hues) was much smaller than that in the prior peak locations ($70.46°$). For one observer (S1) whose blue and yellow unique hue locations deviated from other subjects' settings towards larger hue angles, the corresponding prior peaked at a hue angle close to the average peak location of all subjects' priors. An observer (S6) with a prior peaking at the largest hue angle among subjects did not show pronounced deviations from the other subjects in unique hue categories. Overall, we did not find evidence for covariation between the prior peak location and any of the unique hue locations (Pearson correlation $r = -0.33, p = 0.59$ for unique blue, $r = -0.77, p = 0.12$ for unique yellow, $r = -0.09, p = 0.88$ for unique red, $r = -0.42, p = 0.47$ for unique green). Thus, it is unlikely that the biases we observed could be attributed to categorical effects.

The lack of covariation between priors and unique hue settings may suggest different underlying mechanisms. Recently, Rezeanu et al. (2023) suggested that the basis for unique hues lies in retinal opponency. The model considered by these authors assumed adaptation to equal-energy spectra. However, under changes in macular pigment density, which would have a similar effect as deviations from equal-energy white along the daylight locus, the model's loci of unique blue and unique yellow were fairly stable. Thus, it seems likely that the unique blue and yellow predictions of the model would not have been substantially different if adaptation to some other phase of natural

daylights had been assumed.

Even if the visual systems of different observers are adapted to the same natural stimulus statistics, some interindividual variability is expected. Unique hue percepts are influenced by chromatic context (Klauke & Wachtler, 2016), which suggests that, even if the basis for unique hues is established early in the visual system (Rezeanu et al., 2023), cortical mechanisms may fine-tune color computations for perception. This implies that individual experience during ontogeny may affect perceptual priors, leading to interindividual differences. Moreover, the use of artificial primary spectra in experiments may cause variations in results among individuals. This is because differences in cone spectral sensitivities or pre-receptoral filters can result in different conditions for metamery and thus different results, even when the observers' perceptions of specific broad-band natural spectra would be the same.

4.2. Relation between perceptual variability and bias

The two primary psychophysical measures – perceptual variability and bias – covaried in our experiments: both discrimination thresholds and biases were lowest near the blue-yellow axis and largest orthogonal to the blue-yellow axis. This finding is consistent with previous studies on orientation perception, which have shown a similar relation between threshold and bias minima occurring at cardinal orientations (Tomassini et al., 2010; Girshick et al., 2011).

However, as previous studies have reported, orientation stimuli with high discrimination thresholds or high variability, such as oblique orientations, can also be perceived with minimal bias (Tomassini et al., 2010; Girshick et al., 2011). Wei and Stocker (2017) presented a mathematical description of the relation between variability and bias, suggesting a proportional relationship between bias and the derivative of the square of the discrimination threshold, and found that the relation holds for many visual features, including orientation, motion direction, magnitude, and spatial frequency (Wei & Stocker, 2017). The relationship predicts that bias is minimal at the extrema of discrimination thresholds, with attraction towards the maxima and repulsion bias away from the minima of discrimination thresholds. According to this prediction, one would expect that the bias of perceived hues in our study would show four zero-crossings, corresponding to the number of maxima and minima in the bimodal pattern of discrimination thresholds. Specifically, the hue percept should be biased away from the blue-yellow axis, where discrimination thresholds are minimal, and attracted towards colors with high discrimination thresholds, such as reddish and greenish hues (Fig. S8). However, the measured cross-noise biases showed repulsion from yellow and attraction towards blue.

Potentially, our measurements might have missed to consistently identify some zero crossings, particularly around $157.5°$ where intersubject variability occurred in biases (Fig. 3c) and some subjects showed more than two zero-crossings (Fig. S1). Even if this were the case, the attraction bias around blue in our results is nevertheless inconsistent with the prediction of the Wei-Stocker relation, which would predict that the bias should be repulsive away from blue. An alternative possibility that could explain the deviation of our results from the relation is a strongly skewed likelihood function. Intuitively, one would expect the bias to be zero when the prior of a Bayesian observer is uniformly distributed across the entire range of stimuli. However, the model with a uniform prior predicted non-negligible bias for some of our subjects (Fig. 6, see also S2 and S6 in Fig. S6). These results are likely related to the asymmetry of the likelihood function in the observer model (Wei & Stocker, 2015), which resulted from estimating the likelihood directly from the experimental data by sampling from a measurement distribution, a method also employed by Girshick et al. (2011). While it might be feasible to simultaneously model the likelihood and prior (Stocker & Simoncelli, 2006), we relied on the measurement distribution to ensure reliable likelihoods that captured the perceptual variability for stimuli with specific noise levels. A heavy-

tailed likelihood might lead to a deviation of the posterior from the true stimulus, such that both likelihood shape and prior could contribute to perceptual bias (Stocker & Simoncelli, 2006; Wei & Stocker, 2015; Prat-Carrabin & Woodford, 2021). However, the asymmetric likelihood with a uniform prior generated less accurate predictions than the model with a non-uniform prior (Fig. S6). Thus, the key factor in yielding the systematic bias in our study is likely the non-uniformity of the prior.

Could the marked deviation from the Wei-Stocker relation indicate that the perception of color is governed by fundamentally different principles than other visual features? Wei and Stocker derived their relation under assumptions of efficient coding, specifically, that stimulus encoding maximizes the mutual information between stimuli and sensory representations. How such efficient coding principles would generalize from the univariate case as considered by Wei and Stocker (2017) to higher-dimensional stimulus spaces, like for three-dimensional color space, has not been fully worked out yet (Yerxa et al., 2020). Therefore, it is unclear whether the Wei-Stocker relation applies to univariate manifolds in higher-dimensional stimulus spaces as in our case of a hue circle in three-dimensional color space. Moreover, given the multiple transformations of color signals in the visual system, perceptual judgments in the chromatic domain may be subject to more complex constraints than visual features with simple stimulus correspondence, such as spatial features including orientation or motion direction. Different criteria of efficiency may apply to different aspects or at different stages of visual processing (von der Twer & MacLeod, 2001; Lee et al., 2002; Manning et al., 2024), which would imply deviations from the conditions considered by Wei and Stocker (2017). In particular, sensory signals for color vision are encoded first in a cone-opponent fashion by the retinal circuitry. The resulting representation is the basis for the color space that is commonly used (MacLeod & Boynton, 1979; Derrington et al., 1984), including in our study. Retinal cone opponency decorrelates the photoreceptor signals and thus reduces redundancy (Ruderman et al., 1998; Lee et al., 2002). However, it does not capture the distribution of natural chromatic signals to achieve maximal information (Wachtler et al., 2001; Kellner & Wachtler, 2013). Specifically, retinal cone opponency does not align with the variation of natural illumination, as is reflected by the non-cardinal orientation of the daylight axis in cone-opponent color space (Mollon, 2006). A sensory representation better matched to the distribution of natural chromatic signals appears only at a later stage, by the transformation of color signals in the visual cortex, where the precortically separated cone-opponent signals (Chatterjee & Callaway, 2003) are mixed and a distributed code is achieved (Lennie et al., 1990; Wachtler et al., 2003; Kuriki et al., 2015; Li et al., 2022) that captures the oblique axis of variation of natural daylights (Wachtler et al., 2003; Lafer-Sousa et al., 2012). At least at early cortical stages, neural activity shows features of both kinds of representations (Kaneko et al., 2020). While color appearance judgments are likely based on the cortical representation, perceptual variability may be reasonably assumed to be influenced considerably by the signal-to-noise ratios at precortical stages (Vorobyev & Osorio, 1998). These different influences may result in thresholds and biases inconsistent with the Wei-Stocker relation.

4.3. Hue perceptual non-uniformity and blue-yellow asymmetries

Our study reveals the non-uniformity in perceptual quantities in the present color space. Specifically, discriminability and variability vary in this cone-opponency based color space (Boynton et al., 1986; Krauskopf & Gegenfurtner, 1992; Danilova & Mollon, 2010; Bosten et al., 2015; Klauke & Wachtler, 2015). Our results verified that such non-uniform discriminability also exists for hue ensembles with chromatic noise. Moreover, we found that biases in hue judgments varied with hue, showing minima near blue and yellow, which further reflected the non-uniformity. Notably, the non-uniformity arises not along the cardinal axes of precortical cone opponency, but with respect to the oblique blue-yellow axis that aligns with the variation of natural daylight. The

variance of chromaticity in natural outdoor scenes is also high along this axis (Webster & Mollon, 1997; Webster, 2014; Webster, 2020). This axis has been found special for color vision in many respects, from the distribution of natural chromatic signals (Webster & Mollon, 1997; Wachtler et al., 2001; Webster, 2020) to neural processing (Wachtler et al., 2003; Lafer-Sousa et al., 2012) and perception including discrimination (Danilova & Mollon, 2010; Bosten et al., 2015), color induction (Klauke & Wachtler, 2015), color constancy (Delahunt & Brainard, 2004; Pearce et al., 2014; Gegenfurtner et al., 2015; Lafer-Sousa et al., 2015; Weiss et al., 2017), and, as our results show, priors for hue perception. These prominent features suggest a role of this axis as a perceptual cardinal axis for color vision.

While blue and yellow appear symmetrical, in terms of their similarities in perceptual quantities and the coincidence with the daylight locus (Mollon, 2006; Webster, 2020), the bias in our results was attractive towards blue and repulsive from yellow, confirming asymmetries between blue and yellow (Webster, 2020). A previous study has demonstrated a systematic deviation towards blue when subjects adjusted yoked blue-green hue pairs to achieve an equal perceived mixture of binary hues (Webster et al., 2014). The deviation occurred for unique blue settings and not for other unique hues, which matches the unimodality of the systematic prior revealed in our results. Moreover, the deviation only occurred in the blue-green settings, while no conspicuous bias arose in the mixture consisting of yellow hues, which strongly evidenced asymmetries between blue and yellow.

A special role of blue has been observed previously in color constancy: bluish illumination results in higher color constancy than other chromatic illuminations (Delahunt & Brainard, 2004; Pearce et al., 2014; Winkler et al., 2015; Radonjic et al., 2016; Weiss et al., 2017; Aston et al., 2019). An explanation for this so-called "blue bias" was that the illumination sensitivity threshold is higher for blue than for other colors (Pearce et al., 2014; Radonjic et al., 2016), which would be in line with the hypothesis that the visual system may adapt to the natural environment and be least sensitive to the illumination changes that are most likely to occur (Aston et al., 2019). Additionally, such reduced sensitivity may be attributed to innate physiological factors: short-wavelength-sensitive cones have shown relatively poorer detection of changes in ratios of cone excitations due to illuminant changes (Nascimento & Foster, 1997). Alternatively, given the color distribution of lighting and shadows in natural scenes, the blue bias may emerge from the observer's tendency to infer blue tints as illuminants (Winkler et al., 2015). Although these explanations do not reconcile, most of them commonly imply an environmental account of the blue-yellow asymmetry: color vision may be adapted to natural spectra and expect blue illumination as a dominant feature in natural conditions.

In line with these interpretations, our observer model attributes the blue-yellow asymmetries at the behavioral level to a unimodal prior that peaks at blue. Notably, the unimodal prior outperforms bimodal or uniform priors in predicting the perceptual biases (Fig. S7). Our model is in line with the notion that perception, and in particular color perception, is shaped by the regularities of the sensory environment (Shepard, 1992), but also suggests an asymmetry in natural daylight. As Mollon (2006) has pointed out, the clear sky appears unique blue, which suggests that the light of the sky, resulting from the fundamental physical process of Rayleigh scattering, might provide a stable reference to which color perception is anchored. Thus, in keeping with other Bayesian approaches, our results suggest that human perception internalizes the natural sensory statistics and incorporates prior knowledge into the processing of sensory information.

CRediT authorship contribution statement

Yannan Su: Methodology, Software, Formal analysis, Investigation, Data curation, Visualization, Writing – original draft, Writing – review & editing. **Zhuanghua Shi:** Writing – review & editing, Supervision. **Thomas Wachtler:** Conceptualization, Methodology, Writing – review

& editing, Supervision.

Declaration of competing interest

The authors declare that they have no known competing financial interests or personal relationships that could have appeared to influence the work reported in this paper.

Data availability

The data and code underlying this study is available at G-Node: https://doi.org/10.12751/g-node.rp2ft3.

Acknowledgments

Appendix A. Supplementary data

Supplementary data associated with this article can be found in the online version at https://doi.org/10.1016/j.visres.2024.108406.

References

Akaike, H. (1998). Information theory and an extension of the maximum likelihood principle. In E. Parzen, K. Tanabe, & G. Kitagawa (Eds.), *Selected Papers of Hirotugu Akaike* (pp. 199–213). New York, NY: Springer New York.

Aston, S., Radonjic, A., Brainard, D. H., & Hurlbert, A. C. (2019). Illumination discrimination for chromatically biased illuminations: Implications for color constancy. *Journal of Vision, 19*(3), 15.

Bosten, J. M., Beer, R. D., & MacLeod, D. I. A. (2015). What is white? *Journal of Vision, 15*(16), 5.

Boynton, R. M., Nagy, A. L., & Eskew, R. T., Jr (1986). Similarity of normalized discrimination ellipses in the constant-luminance chromaticity plane. *Perception, 15*(6), 755–763.

Brainard, D. H., Longère, P., Delahunt, P. B., Freeman, W. T., Kraft, J. M., & Xiao, B. (2006). Bayesian model of human color constancy. *Journal of Vision, 6*(11), 1267–1281.

Chatterjee, S., & Callaway, E. M. (2003). Parallel colour-opponent pathways to primary visual cortex. *Nature, 426*(6967), 668–671.

Danilova, M. V., & Mollon, J. D. (2010). Parafoveal color discrimination: a chromaticity locus of enhanced discrimination. *Journal of Vision, 10*(1), 4.1–9.

Delahunt, P. B., & Brainard, D. H. (2004). Does human color constancy incorporate the statistical regularity of natural daylight? *Journal of Vision, 4*(2), 57–81.

Derrington, A. M., Krauskopf, J., & Lennie, P. (1984). Chromatic mechanisms in lateral geniculate nucleus of macaque. *The Journal of Physiology, 357*, 241–265.

Ernst, M. O., & Banks, M. S. (2002). Humans integrate visual and haptic information in a statistically optimal fashion. *Nature, 415*(6870), 429–433.

Gao, F., & Han, L. (2012). Implementing the Nelder-Mead simplex algorithm with adaptive parameters. *Computational Optimization and Applications, 51*(1), 259–277.

Gegenfurtner, K. R., Bloj, M., & Toscani, M. (2015). The many colours of 'the dress'. *Current Biology, 25*(13), R543–R544.

Girshick, A. R., Landy, M. S., & Simoncelli, E. P. (2011). Cardinal rules: Visual orientation perception reflects knowledge of environmental statistics. *Nature Neuroscience, 14*(7), 926–932.

Glasauer, S., & Shi, Z. (2022). Individual beliefs about temporal continuity explain variation of perceptual biases. *Scientific Reports, 12*(1), 10746.

Green, D. M., & Swets, J. A. (1966). *Signal detection theory and psychophysics*. New York: Wiley.

Hansen, T., Walter, S., & Gegenfurtner, K. R. (2007). Effects of spatial and temporal context on color categories and color constancy. *Journal of Vision, 7*(4), 2.

Kaiser, P. K., & Boynton, R. M. (1996). *Human color vision*. Washington: Optical Society of America.

Kaneko, S., Kuriki, I., & Andersen, S. K. (2020). Steady-State visual evoked potentials elicited from early visual cortex reflect both perceptual color space and Cone-Opponent mechanisms. *Cerebral Cortex Communications, 1*(1), Article tgaa059.

Kellner, C. J., & Wachtler, T. (2013). A distributed code for color in natural scenes derived from center-surround filtered cone signals. *Frontiers in Psychology, 4*(661), 1–11.

Kersten, D., Mamassian, P., & Yuille, A. (2004). Object perception as Bayesian inference. *Annual Review of Psychology, 55*, 271–304.

Klauke, S., & Wachtler, T. (2015). "Tilt" in color space: Hue changes induced by chromatic surrounds. *Journal of Vision, 15*(13), 17,1–11.

Klauke, S., & Wachtler, T. (2016). Changes in unique hues induced by chromatic surrounds. *Journal of The Optical Society of America A: Optics, Image Science, and Vision, 33*(3), A255–9.

Knill, D. C., & Pouget, A. (2004). The Bayesian brain: The role of uncertainty in neural coding and computation. *Trends in Neurosciences, 27*(12), 712–719.

Körding, K. P., & Wolpert, D. M. (2004). Bayesian integration in sensorimotor learning. *Nature, 427*(6971), 244–247.

Krauskopf, J., & Gegenfurtner, K. (1992). Color discrimination and adaptation. *Vision Research, 32*(11), 2165–2175.

Kuriki, I., Sun, P., Ueno, K., Tanaka, K., & Cheng, K. (2015). Hue selectivity in human visual cortex revealed by functional magnetic resonance imaging. *Cerebral Cortex, 25*, 4869–4884.

Lafer-Sousa, R., Hermann, K. L., & Conway, B. R. (2015). Striking individual differences in color perception uncovered by 'the dress' photograph. *Current Biology, 25*(13), R545–546.

Lafer-Sousa, R., Liu, Y. O., Lafer-Sousa, L., Wiest, M. C., & Conway, B. R. (2012). Color tuning in alert macaque V1 assessed with fMRI and single-unit recording shows a bias toward daylight colors. *Journal of the Optical Society of America A: Optics, Image Science, and Vision, 29*(5), 657–670.

Lee, T.-W., Wachtler, T., & Sejnowski, T. J. (2002). Color opponency is an efficient representation of spectral properties in natural scenes. *Vision Research, 42*(17), 2095–2103.

Lennie, P., Krauskopf, J., & Sclar, G. (1990). Chromatic mechanisms in striate cortex of macaque. *The Journal of Neuroscience, 10*(2), 649–669.

Li, P., Garg, A. K., Zhang, L. A., Rashid, M. S., & Callaway, E. M. (2022). Cone opponent functional domains in primary visual cortex combine signals for color appearance mechanisms. *Nature Communications, 13*(1), 6344.

MacLeod, D. I., & Boynton, R. M. (1979). Chromaticity diagram showing cone excitation by stimuli of equal luminance. *Journal of The Optical Society of America A: Optics, Image Science, and Vision, 69*(8), 1183–1186.

Manning, T. S., Alexander, E., Cumming, B. G., DeAngelis, G. C., Huang, X., & Cooper, E. A. (2024). Transformations of sensory information in the brain suggest changing criteria for optimality. *PLoS Computational Biology, 20*(1), e1011783.

Maule, J., & Franklin, A. (2015). Effects of ensemble complexity and perceptual similarity on rapid averaging of hue. *Journal of Vision, 15*(4), 6.

Maule, J., Witzel, C., & Franklin, A. (2014). Getting the gist of multiple hues: metric and categorical effects on ensemble perception of hue. *Journal of The Optical Society of America A: Optics, Image Science, and Vision, 31*(4), A93–102.

Mollon, J. (2006). Monge: The Verriest lecture, Lyon, July 2005. *Visual Neuroscience, 23*(3–4), 297–309.

Nascimento, S. M., & Foster, D. H. (1997). Detecting natural changes of cone-excitation ratios in simple and complex coloured images. *Proceedings of the Royal Society B: Biological Sciences, 264*(1386), 1395–1402.

Nascimento, S. M. C., Ferreira, F. P., & Foster, D. H. (2002). Statistics of spatial cone-excitation ratios in natural scenes. *Journal of The Optical Society of America A: Optics, Image Science, and Vision, 19*(8), 1484–1490.

Pearce, B., Crichton, S., Mackiewicz, M., Finlayson, G. D., & Hurlbert, A. (2014). Chromatic illumination discrimination ability reveals that human colour constancy is optimised for blue daylight illuminations. *PLoS One, 9*(2), e87989.

Peirce, J., Gray, J. R., Simpson, S., MacAskill, M., Höchenberger, R., Sogo, H., Kastman, E., & Lindeløv, J. K. (2019). PsychoPy2: Experiments in behavior made easy. *Behavior Research Methods, 51*(1), 195–203.

Prat-Carrabin, A., & Woodford, M. (2021). Bias and variance of the Bayesian-mean decoder. In M. Ranzato, A. Beygelzimer, Y. Dauphin, P. S. Liang, & J. W. Vaughan (Eds.), *Advances in Neural Information Processing Systems* (Vol. 34, pp. 23793–23805). Curran Associates Inc.

Radonjic, A., Pearce, B., Aston, S., Krieger, A., Dubin, H., Cottaris, N. P., Brainard, D. H., & Hurlbert, A. C. (2016). Illumination discrimination in real and simulated scenes. *Journal of Vision, 16*(11), 2.

Rezeanu, D., Neitz, M., & Neitz, J. (2023). From cones to color vision: A neurobiological model that explains the unique hues. *Journal of The Optical Society of America A: Optics, Image Science, and Vision, 40*(3), A1–A8.

Ruderman, D., Cronin, T., & Chiao, C. (1998). Statistics of cone responses to natural images: implications for visual coding. *Journal of The Optical Society of America A: Optics, Image Science, and Vision, 15*(8), 2036–2045.

Shepard, R. N. (1992). The perceptual organization of colors: An adaptation to regularities of the terrestrial world?. In J. H. Barkow (Ed.), *The adapted mind: Evolutionary psychology and the generation of culture* (Vol. 666, pp. 495–532) New York: Oxford University Press.

Shi, Z., & Burr, D. (2016). Predictive coding of multisensory timing. *Current Opinion in Behavioral Sciences, 8*, 200–206.

Shi, Z., Church, R. M., & Meck, W. H. (2013). Bayesian optimization of time perception. *Trends in Cognitive Sciences, 17*(11), 556–564.

Stocker, A. A., & Simoncelli, E. P. (2006). Noise characteristics and prior expectations in human visual speed perception. *Nature Neuroscience, 9*(4), 578–585.

Stockman, A., & Sharpe, L. T. (2000). The spectral sensitivities of the middle- and long-wavelength-sensitive cones derived from measurements in observers of known genotype. *Vision Research, 40*(13), 1711–1737.

Su, Y., Wachtler, T., & Shi, Z. (2023). Reference induces biases in late visual processing. *Scientific Reports, 13*(1), 18624.

Teufel, H. J., & Wehrhahn, C. (2000). Evidence for the contribution of S cones to the detection of flicker brightness and red-green. *Journal of The Optical Society of America A: Optics, Image Science, and Vision, 17*(6), 994–1006.

Tomassini, A., Morgan, M. J., & Solomon, J. A. (2010). Orientation uncertainty reduces perceived obliquity. *Vision Research, 50*(5), 541–547.

Vattuone, N. and Samengo, I. (2023). The predictive power of the geometry of colour space. https://doi.org/10.1101/2023.09.16.557954. bioRxiv preprint.

Vattuone, N., Wachtler, T., & Samengo, I. (2021). Perceptual spaces and their symmetries: The geometry of color space. *Mathematical Neuroscience and Applications, 1*.

Virtanen, L. S., Olkkonen, M., & Saarela, T. P. (2020). Color ensembles: Sampling and averaging spatial hue distributions. *Journal of Vision, 20*(5), 1.

von der Twer, T., & MacLeod, D. I. (2001). Optimal nonlinear codes for the perception of natural colours. *Network, 12*(3), 395–407.

von Helmholtz, H. (1867). Handbuch der physiologischen Optik. *Voss*.

Vorobyev, M., & Osorio, D. (1998). Receptor noise as a determinant of colour thresholds. *Proceedings of the Royal Society B: Biological Sciences, 265*(1394), 351–358.

Wachtler, T., Lee, T. W., & Sejnowski, T. J. (2001). Chromatic structure of natural scenes. *Journal of The Optical Society of America A: Optics, Image Science, and Vision, 18*(1), 65–77.

Wachtler, T., Sejnowski, T. J., & Albright, T. D. (2003). Representation of color stimuli in awake macaque primary visual cortex. *Neuron, 37*(4), 681–691.

Webster, J., Kay, P., & Webster, M. A. (2014). Perceiving the average hue of color arrays. *Journal of The Optical Society of America A: Optics, Image Science, and Vision, 31*(4), A283–92.

Webster, M. (2014). Environmental influences on color vision. In R. Luo (Ed.), *Encyclopedia of Color Science and Technology* (pp. 1–6). Berlin, Heidelberg: Springer Berlin Heidelberg.

Webster, M. A. (2020). The Verriest lecture: Adventures in blue and yellow. *Journal of The Optical Society of America A: Optics, Image Science, and Vision, 37*(4), V1–V14.

Webster, M. A., Miyahara, E., Malkoc, G., & Raker, V. E. (2000). Variations in normal color vision. II. Unique hues. *Journal of The Optical Society of America A: Optics, Image Science, and Vision, 17*(9), 1545–1555.

Webster, M. A., Mizokami, Y., & Webster, S. M. (2007). Seasonal variations in the color statistics of natural images. *Network, 18*(3), 213–233.

Webster, M. A., & Mollon, J. D. (1997). Adaptation and the color statistics of natural images. *Vision Research, 37*(23), 3283–3298.

Wei, X.-X., & Stocker, A. A. (2015). A Bayesian observer model constrained by efficient coding can explain 'anti-Bayesian' percepts. *Nature Neuroscience, 18*(10), 1509–1517.

Wei, X.-X., & Stocker, A. A. (2017). Lawful relation between perceptual bias and discriminability. *Proceedings of the National Academy of Sciences of the United States of America, 114*(38), 10244–10249.

Weiss, D., Witzel, C., & Gegenfurtner, K. (2017). Determinants of colour constancy and the blue bias. *i-Perception, 8*(6), 2041669517739635.

Wichmann, F. A., & Hill, N. J. (2001). The psychometric function: I. Fitting, sampling, and goodness of fit. *Perception & Psychophysics, 63*(8), 1293–1313.

Winkler, A. D., Spillmann, L., Werner, J. S., & Webster, M. A. (2015). Asymmetries in blue-yellow color perception and in the color of 'the dress'. *Current Biology, 25*(13), R547–R548.

Witzel, C., & Gegenfurtner, K. R. (2013). Categorical sensitivity to color differences. *Journal of Vision, 13*(7), 1.

Wyszecki, G., & Stiles, W. S. (1982). *Color science: Concepts and methods, quantitative data and formulae*. New York: Wiley.

Yerxa, T. E., Kee, E., DeWeese, M. R., & Cooper, E. A. (2020). Efficient sensory coding of multidimensional stimuli. *PLoS Computational Biology, 16*(9), e1008146.